Control of the alumino-silico-phosphate geopolymers properties and structures by the phosphorus concentration

Virginie Mathivet, Jenny Jouin, Michel Parlier, Sylvie Rossignol

CONTROL OF THE ALUMINO-SILICO-PHOSPHATE GEOPOLYMERS PROPERTIES AND STRUCTURES BY THE PHOSPHORUS CONCENTRATION

V. Mathivet[1,2], J. Jouin[1], M. Parlier[2] and S. Rossignol[1]

[1] IRCER: Institut de Recherche sur les Céramiques (UMR-CNRS 7315), 12 rue Atlantis, 87068 Limoges Cedex, France.

[2] ONERA: Office National d'Etudes et de Recherches Aérospatiales, 29 Avenue de la Division Leclerc, 92320 Châtillon, France.

■ corresponding author: sylvie.rossignol@unilim.fr, tel.: 33 5 87 50 25 64

Phosphoric acid	Water content	Al/P
Working properties	Various networks	Geopolymer

Abstract

Acid-based geopolymers are interesting materials, as they usually present higher mechanical and thermal properties than their alkali-based counterparts do, but they are difficult to use for complex shapes due to the high viscosity of their reactive mixture. This can be overcome by the addition of water in the formulation. In this study, geopolymers have been synthesized from metakaolin and phosphoric acid with variable [P] concentration (by a modification of either the water content or Al/P ratio). Measurements of the viscosity, density and consolidation times have been performed on reactive mixtures differentiated by their water content. Furthermore, a study of the geopolymers' microstructure and mechanical properties confirmed their evolution with [P]. Finally, a characterization by thermal and structural analyzes of their structure (Fourier transform infrared spectroscopy and X-ray diffraction), have been carried out in order to assess the influence of the water content on the different amorphous networks. It appears that the addition of water influences the structure of the material, as it leads to the formation of new

amorphous networks. More specifically, for Al/P = 1 and variable water amounts, the networks are mainly based on the coexistence of Al-O-P with an hydrated silica network, while for variable Al/P, the Al-O-P network coexists with the unreacted metakaolin. In addition, it seems that all the properties are governed by the parameter $n_P/n_{Al} + n_{H_2O}$.

I. Introduction

Over the past decades, numerous researches have been conducted on geopolymer materials. These materials indeed combine interesting mechanical properties, reduced CO_2 footprint and high chemical resistance compared to Portland cements, paving the way to new applications ranging from environmentally friendly construction to the encapsulation of toxic waste [1, 2]. These materials are synthesized from the dissolution of an aluminosilicate source into an alkaline solution. The resulting oligomers $Si(OH)_4$ and $Al(OH)_4^-$ then polycondensate to form amorphous three-dimensional networks. Their working properties have been widely studied, showing that they can be adjusted by the reactivity of the aluminosilicate sources towards alkali activators through their reaction mechanisms [3]. More recently, a new synthesis process, using an acidic activation solution, has been explored. This path seems promising as the resulting materials present improved mechanical properties [4, 5]. An acid-based geopolymer formation starts with the dissolution of an aluminosilicate source into an acid (usually orthophosphoric acid) leading to the release of Al^{3+} ions, which then polycondense with the phosphorous entities to form three-dimensional hydrated aluminophosphate networks [6]. The hydrated silica still remaining after the release of those Al^{3+} ions can then form some additional silicate networks, that may react with some of the remaining phosphorous entities, thus forming Si-O-P bonds [6, 7]. As for geopolymers in alkali medium, previous studies were carried out to understand the influence of the aluminosilicate sources, the activation solution and the consolidation temperature on the structure and working properties of acid-based geopolymers [8, 9]. For example, Thakouté *et al.* have shown that the addition of gibbsite in a

geopolymer negatively affects its properties [10]. The dilution of the concentrated phosphoric acid leads to an improvement of the mechanical properties up to a concentration of 10 M then a decrease was observed simultaneously with the existence of several networks in acid geopolymer [11] In this study the porosity values did not change with the concentration of hardeners. Another publication has stated that the best mechanical properties, associated with a low porosity of 8 %, are also achieved for [P] equal to 10 M. [12] Another work on the effect of the P/Al ratio demonstrated a maximum mechanical resistance for P/Al = 1 [13]. In addition, different phosphorus concentrations have been studied to control the viscosity as well as the setting time. Thus, Dong *et al.* have demonstrated that the viscosity vary from 3 to 7 MPa.s. [12] The viscosity of the acid-based geopolymers' reactive mixture still tends to be high, which is detrimental for industrial applications, such as the production of geopolymer-based composites. Thus, the addition of water in the original reactive mixture can be necessary to improve the rheological properties of the mixture (various Al/P).

The dissolution of the metakaolin in an acidic medium contributes to the overall kinetic control of the geopolymerization reaction [14], being dependent on the activation energy, the temperature and the diffusion mechanisms. The difficulty to fully dissolve the metakaolin in the acid may then lead to the leaching of most of the octahedral Al^{3+} cations and to the formation of amorphous and highly porous silica-based solids [15], resulting in a high level of inhomogeneity's in the final product. It is thus fundamentally valuable for the production of new materials, that the equilibrium of the system is understood and established in order to control the dissolution of species. Moreover, in order to control the dissolution of metakaolin, it is essential to control both the degree of polymerization of phosphoric acid as well as the chemical mechanism of polycondensation reaction [10, 16]. An example of application for these diluted geopolymers is the production of textile reinforced by phosphate binders, where an investigation is necessary, in particular to understand the water related phases of the process,

as it can be absorbed during the various reaction [17] This concerns in particular the amount of water involved in the formation mechanisms of geopolymeric materials, including the effect of water addition on the structure and mechanical properties of acid-based geopolymers.

Our study thus addressed the influence of P concentration through water addition on the reactive mixture, the structure and working properties of acid-based geopolymers. First, the effect of the formulation of the reactive mixtures on the working properties (viscosity, consolidation time), and the mechanical properties of the consolidated materials, were characterized in order to be able to adjust the water content to the selected manufacturing process and compared to existing data. The bonding-type of water and its location in the material were then identified by structural analyses. Finally, the evolution of the networks in the material was monitored as a function of the water addition.

II. Experimental part

1. Raw materials and sample preparation

The synthesis of the reference geopolymer was described in a previous study [6], using a metakaolin produced by Imerys with a Si/Al ratio equal to 1 as the aluminosilicate source, whose characteristics and reactivity have been studied by Gharzouni *et al.* [18], and a 85 wt% pure phosphoric acid produced by VWR. During the synthesis, the phosphoric acid has been first diluted in distilled water to reach the selected water content and mixed with the metakaolin until reaching an Al/P ratio equal to 1, this reactive mixture being then poured in a sealed container and cured at 70°C for 72 h.

In this study, the influence of the water content on the reactive mixture has been studied by synthetizing two series of samples. The first one has been obtained by adding water to the reference composition, originally containing 0.45 mol % of water, and called R [6], up to a maximum of 0.68 mol %. The notation of those samples has been defined as R-x, x being the

ratio of the molar percentage of added water over the reference one. The second series has been synthesized by modifying the Al/P composition of the samples and adjusting the quantity of added water to the metakaolin water demand. **Figure 1** shows the ternary diagram regrouping all those compositions. As it can be seen, the compositions of the samples belong to a small range of the diagram, which induce a phosphorus concentration in the range 3.5 – 7.23 M.

2. Characterization techniques

The viscosity of the reactive mixture was characterized with a BROOKFIELD DV2T apparatus and measured up to 2000 Pa.s using a LV-04 mobile. The speed of the spindle was in the range of 10 to 100 rpm, depending on the viscosity of the mixture, which density was determined based on the measurement of the mass of a cubic centimeter.

The Fourier Transform Infrared (FTIR) spectra were recorded and analyzed on a PERKIN-ELMER Frontier apparatus and its software, in transmission mode between 400 and 4000 cm^{-1} with 4 scans and a 4 cm^{-1} resolution. Moreover, KBr pellets were elaborated for all the samples.

The X-ray diffraction (XRD) patterns have been recorded with a Bruker D8 Advance diffractometer using a CuK_{α} radiation. The acquisitions have been carried out with a 2θ-angle in the range of 5 to 60° with a 0.02° step size and a 50 s equivalent time per step. The decomposition of the contributions from the different amorphous networks has been conducted using the Peakoc software [19], and the refinement between 5 and 60° using Voigt functions taking into account the $CuK_{\alpha 1}$ and $CuK_{\alpha 2}$ wavelengths.

The thermal analyses have been realized on an SDT Q600 apparatus from TA Instrument. The measurements have been performed in platinum crucibles under a flow of dry air (100 $mL.min^{-1}$) with a 5°$C.min^{-1}$ slope up to 1000 °C.

The measurements of compressive strength have been carried out on a Lloyd EZ20 universal testing machine with a 0.5 mm.min^{-1} crosshead speed. Seven days after consolidation, five geopolymers with a 15 mm diameter and a 30 mm height have been selected for each composition, ground to obtain plane and parallel surfaces and analyzed. The specific mass has been determined prior to the measurement on the ground samples (Φ/H = 0.5).

Measurements of the volume fraction of porosity have been realized using Archimedes' method [20], thus giving access to the open porosity. The samples have been preliminary vacuum packaged, and then progressively covered with water while kept under vacuum. Weight measurements at dry (m_{dry}), immersed in water (m_{imm}) and saturated of water (m_{sat}) stages have been used to determine the porosity, following the equation: $Porosity\ (\%) = \frac{m_{sat}-m_{dry}}{m_{sat}-m_{imm}}$.

III. Results

1. Influence of the water addition for Al/P = 1

1.1. Reactive mixtures

In order to study the influence of the water addition on the process parameters, the viscosity and setting time of the various compositions R-x have been plotted as a function of the water content in **figure 2**. The reference sample displays an initial viscosity of 30 Pa.s and needs 46 h to consolidate. The viscosity of the reactive mixtures then decreases with the addition of water, whereas the setting time increases. More precisely, the viscosity drops sharply from 30 to 2 Pa.s between 0.45 and 0.60 mol % of water. At higher water contents, the viscosity decreases slowly down to 0.6 Pa.s at 0.68 mol % of water. This general trend is due to the reduction of the solid/liquid volume fraction of the reactive mixture, diminishing the friction between the particles. The setting time remains constant at around 46 h between 0.45 and 0.55 mol %; however from 0.60 mol % on, a steep increase occurs, leading to a maximum setting time of 69 h for 0.68 mol % of water. This evolution can be explained by the dilution of the

reactive species forming for a great part the geopolymer network [6, 12], as low phosphorus and aluminum concentrations reduce the encounter probability of those species.

All these data underline that processing and manufacturing parameters, such as the viscosity of the reactive mixture and its setting time, may be adjusted by modifying the water content of the formulations with Al/P =1. However, the influence of the water content on the geopolymer structure has yet to be investigated.

1.2. Consolidated materials

In order to evaluate the amount and type of water issued from the polycondensation reaction, thermal analyses of the samples were conducted; as an illustration, **figure 3Aa** presents the thermogram (20-240 °C) of the sample R-1.2, which is representative of the measurements carried out on similar materials [6]. Three endothermic phenomena, corresponding to the temperatures ranges T < 110°C, 110 < T < 220°C and T > 220°C and related to weight losses, are identified and labeled I, II and III, respectively. The first weight loss (I) is attributed to the evaporation of physisorbed water. Then, two smaller weight losses (IIa and IIb) are observed between 110 and 240°C, and are associated with the dehydration of hydrated phases [9, 21]. **Figure 3Ab** compares the behavior of three of the samples (R, R-1.2 and R-1.5). As it can be observed, the thermograms present the same general evolution, save for the weight loss during step I, where the physisorbed water evaporates before 100°C. In order to investigate the distribution of physisorbed and chemisorbed water inside the samples, **figure 3B** displays the weight loss from steps I and II, as well as the total weight loss in the temperature range 25 to 1000°C. This shows that the evolution of the total weight loss occurring after the addition of water is mainly due to the increase of the weight loss from step I. It appears that the excess of water introduced does not participate much to the polycondensation reactions. Thus,

the amount of water used for the geopolymer formation (step II) is rather stable and the rest remains as physisorbed water.

Moreover, in order to determine the influence of water on the inner structure of the consolidated geopolymer, FTIR spectroscopy measurements have been carried out and are presented in **figure 4A** (OH entities) and **figure 4B** (silicon and aluminophosphate species) for samples R, R-1.2 and R-1.5. The same bands are identified on all the samples, though differing in intensity. More specifically, the bands located at 3680, 3570, 3440, 3350 and 3240 cm^{-1} are respectively attributed to the following bonds: P-OH, SiOH (asym and sym), OH – $AlPO_4$ and bonded H_2O [11, 22, 23]. The contributions around 1640 cm^{-1} are assigned to the bending of P-OH and water molecules, those at 1220 (w), 1155 (w), 1095 and 920 cm^{-1} to the stretching of P-O from hydrated aluminophosphates [24, 25], and the one at 800 cm^{-1} is related to the bending of Si-O-Si bonds. The bands in the range 1300-500 cm^{-1} do not evolve significantly with the addition of water and their identification remains complex due to the presence of silicate species in the same region. As it has been outlined by Mathivet *et al.* [6], aluminophosphate and Si-OH networks mainly form the geopolymer, which is confirmed here. Their formation takes place regardless of the water content, and in each case consumes the same amount of water. Then, the water in excess, which is not consumed during the geopolymer formation, leads to the presence of hydrated phases or physorbed phases. This last point is in agreement with the increasing amount of physisorbed water observed during the thermal analyses and reported in other works [5, 10, 12, 13]. These results outline that an increase in the water content results in the formation of several hydrated compounds or physisorbed water.

The compressive strength and porosity of the consolidated geopolymers are also sensitive to the water content, as shown in **figure 5**. As a matter of fact, with the addition of water in the reactive mixture, the compressive strength decreases as the porosity increases. The compressive strength values indeed drop from 80 to 11 MPa for a phosphorus concentration of

6.5 to 4.5 M, these values being agreement with the literature [11]. The decrease of the mechanical properties with water or with the decrease of the phosphorus concentration is associated with the formation of pores in the microstructure as it can observed in **figure 5**, and in accordance with literature data [11, 14]. The addition of water indeed leads to a disordered microstructure and the presence of hydrated networks, weakening the mechanical properties.

2. Influence of the composition: Al/P ratio

As stated previously, another way to reduce the viscosity of the reactive mixtures lies in a slight modification of their composition. To emphasize this point, several formulations with Al/P ratios ranging from 0.9 to 1.8 have been synthetized at a constant solid to liquid ratio, and compared to the previous samples, belonging to the same range of [P] concentration, the shaping of the samples being highly dependent on the properties of the reactive mixture. After the characterization of their properties, the study focused on the local networks forming the samples.

The viscosity recorded in **table 1** decreases with the addition of water for Al/P = 1, as already seen, and follows the same trend when Al/P increases. This evolution is strongly linked to the amount of water present in the reactive mixture in both cases, as an increase in Al/P is accompanied by an increase in the molar ratio of water. On the other hand, the setting time does not follow the same evolution. It slowly increases with the addition of water for Al/P = 1, and the evolution is inversely proportional to the water content of the reactive mixture, which may be explained by the evolution of the species concentration in the reactive mixture [26]. For both systems, the viscosity drops due to the electrostatic repulsion [27] reducing the species' mobility originating from the addition of water and the change of the PO_4 entities [16]. Concerning the consolidation of the samples, for Al/P = 1, the dilution directly limits the polycondensation reactions, which may be the cause of the increased setting time. In the case

of a variable Al/P, the growing presence of free reagents in the mixture (especially aluminum) compensates the dilution effect induced by the water, thus leading to a shorter setting time.

Figure 6 shows the mechanical strength as well as some porosity for the different samples. Whatever the series of samples considered, an increase of the molar number of water introduced leads to a decrease in the compressive strength as shown in **figure 6A**, linked to the raise of the porosity observed (**figure 6B**). However, another factor may also influence this degradation, as the reactive species tend to be more diluted with the addition of water, thus reducing the chemical potential. In addition, the reactivity of aluminate species is dependent on their charge and size [28]. The mechanism of formation of oligomers can thus be modified, giving birth to different local networks based on aluminum phosphate, hydrated silica or other hydrated phases, as it was observed in alkaline medium [29, 30. 31]. These networks can display different values of specific mechanical resistance, leading to a variation of the compressive resistance of the samples depending on their distribution. Finally, some samples were heated at 250°C for 2 hours, heating during which the amount of water lost was measured in order to evaluate its location in the samples (**figure 6C**). The evolution of the weight loss reveals the existence of poral water and of some chemisorbed water due to hydrated phases [32], suggesting that its excess remains physisorbed, which generates a higher porosity. After the thermal treatment (**Figure 6D**), the porosity still increases with the amount of water introduced, but it is significantly higher than its value before drying the sample. This confirms the presence of water in both open and closed porosity, which fractures the sample during heating, leaving access to a higher fraction of open pores after treatment. Similar results have been established, showing that the phosphorus concentration, water amount and Al/P control the properties of the geopolymers. However, it is also necessary to understand the influence of the availability of reactive aluminous or phosphate species on these materials.

IV. Discussion: modification of the networks

It has been shown that a variable water content introduced into the reactive mixtures modifies the properties of materials, and leads to structural modifications at the local network level as well, including the types of bonds and their distribution. Moreover, many hydrated phases can coexist in this type of material in the temperature range 25-250°C [6]. To corroborate these hypotheses, the presence of amorphous networks in the geopolymers was studied by XRD; the diagrams measured for various Al/P and Al/P = 1 with different amounts of water are presented in **figures 7A** and **B**, respectively. As previously observed [6], they all display a broad contribution centered at 27°, as well as some peaks attributed to crystalline anatase (JCPDS: 01-071-1166) and quartz (JCPDS: 00-046-1045). These crystalline phases were identified in the metakaolin and are not modified by the geopolymerization process [33]. Although the main contribution is observed in all the samples, it shows some minor differences in its shape from one sample to another, suggesting the presence of several amorphous networks. They were identified in our previous study [7] and can be described as follows. The first contribution, thereafter called S, is located at the fixed position of 21.9° and assigned to an amorphous silica network [34]. The second one, thereafter called G, is located at an average position of 27.9° and is attributed to the formation of the amorphous geopolymer network, mainly constituted of hydrated aluminophosphates [25]. Furthermore, some diagrams in **figures 7A** and **B** show a low intensity dome at low diffraction angles (peak 1), which is assigned to an hydrated silica network [35, 36]. It is then interesting to note that for the samples containing the most water, *i.e.* R-1.4 and R-1.5 (**figure 7B**), additional contributions appear at higher angles (peaks 2 and 3). The same phenomenon occurs for variable Al/P samples, but in this case the sole peak 3 was identified. Those two contributions have yet to correlate with a type of amorphous network, as XRD does not give sufficient data for this, but they nonetheless confirm the participation of new amorphous networks in the samples with the highest content of water.

The positions, intensities and broadening of the amorphous contributions identified in the XRD diagrams were thus refined, and the details of those analyses are gathered in the supplementary material. The evolution of the relative intensities I_G/I_S gives an accurate indication about the level of geopolymerization in the sample, as stated in a previous work [6]. In the present work, I_G/I_S is also clearly related to the water content of the reactive mixture, as presented in **figure 8**. The samples with a variable Al/P present a two-step evolution. First, for Al/P in the range of 0.9 to 1.1, the diagram shows a relatively small variation, which implies that the geopolymer network is not significantly modified for these compositions. However, with an increasing Al/P ratio, and subsequently an increasing amount of water, I_G/I_S decreases sharply, indicating that the original geopolymer network is less present in these samples. This occurs in conjunction with the appearance of the signature from a new network (peak 3) and the loss of peak 1, related to hydrated silica. Thus, this new undefined network seems to replace at least partially the original geopolymer's one. When raising the water amount in the sample while keeping Al/P constant, I_G/I_S decreases more regularly for the R – R-1.3 compositions. This indicates that the geopolymer network prevails less and less, although its intensity is still high. For the highest content of water, i.e. R-1.4 and R-1.5, the signatures of new networks (peaks 2 and 3) appear, and the intensity of G decreases simultaneously, reaching its lowest value. The relative intensity of the geopolymer network is similar for variable Al/P and variable water amount, though modifying the water addition in a sample with Al/P = 1 gives a better control on the intensity of the contribution assigned to the geopolymer network, as there is no threshold effect in this case.

Finally, in order to identify the networks that appear to replace the original Al-O-P-based one, an FTIR study has been carried out to investigate the type of entities present in each formulation. Thus, the evolution of the intensities of some characteristic bands from phosphates, silicate and aluminate networks have been studied, and the full spectra are given in

supplementary material. These networks are dependent on the composition of the reactive mixture, which is a combination of the molar P/Al ratio and the amount of available water, which double influence has been expressed in the parameter (nP/nAl) + nH_2O. To justify the use of this new parameter, the water content determined by thermal analysis (data are provided in supplementary files) has been plotted as a function of the expression (nP/nAl) + nH_2O and is displayed in **figure 9**. The linear variation observed suggests a strong correlation that outlines the ability of the samples to trap water.

Figure 10 shows the evolution of the different bands' intensity as a function of the parameter (nP/nAl) + nH_2O. As stated previously, at least three types of networks (aluminophosphate, silicophosphate and undissolved silica hydrates) may follow the reaction between the metakaolin and the phosphoric acid. The contributions attributed to the silicates (SiO-H asym and sym) at 3530 - 3440 cm^{-1} and to the bound water at 3240 cm^{-1} are reported in **figure 10A**. It reveals that the contribution of silanols increases with a high amount of water. This is related to the availability of water in the reactive mixture, which can react with the metakaolin. Furthermore, for low values of (nP/nAl) + nH_2O (corresponding to high Al/P), a higher amount of undissolved metakaolin in the system is associated with its lower hydration and therefore the decrease of the contribution from silanols [37]. However, the evolution related to the bound water does not follow the exact same trend, as its intensity ratio reaches its highest value for the reference composition. It suggests that increasing the amount of water in the reactive mixture leads to the presence of more physisorbed water, however it does not seem to affect the chemisorbed one. This may be related to the formation of hydrated phases of probably different chemical composition, as suggested from XRD in **figure 8**, and to the loss of the hydrated silica contribution. Similarly, **figure 10B** gathers the contributions of the phosphate-based networks at 1220 cm^{-1} (ν Al-O-P), 1095 and 1155 cm^{-1} (asym and sym ν P-O) as a function of (nP/nAl) + nH_2O. The intensity of the band at 1220 cm^{-1}, corresponding to Al-O-P

bonds, tends to decrease, especially for the highest amounts of water. This can be explained by a dilution effect that disadvantages the reaction between aluminum and phosphorus species. This was also observed previously by XRD, as the relative intensity of the I_G contribution is mostly connected to the presence of Al-O-P networks. Moreover, this dilution effect seems to be expanded to the signature of the P-O bonds. Finally, the evolution of the contributions mainly related to the phosphate lattice, such as hydrated Al-O-P at 3350 cm^{-1}, υ PO-H at 1640 cm^{-1}, and υ Si-O-P at 1206 cm^{-1}, are displayed in **figure 10C**. The bands for hydrated aluminum phosphates and PO-H are almost constant, indicating that these networks are formed regardless of the formulation of the reactive mixture. Concerning the band allocated to the Si-O-P network (1206 cm^{-1}), its relative intensity diminishes when (nP/nAl) + nH_2O increases. This can be explained by the preferential formation of aluminophosphate entities [38], when the species are available. Besides, for higher Al/P ratios, the presence of large amounts of unreacted metakaolin and undissolved silica is higher, and the molecular interactions will thus favor the formation of Si-O-P and Si-O-Al bonds [39].

V. Conclusion

This study focused on the influence of the initial water content on the structure and working properties of phosphoric acid-based geopolymers. The addition of water to the reactive mixtures leads to a sharp decrease of its viscosity, as well as a modification of its setting time, *i.e.* a longer setting time in the case of a dilution with Al/P = 1 and a shorter one when increasing Al/P. Moreover, the resulting consolidated materials are characterized by a deterioration of their mechanical properties, along with a higher level of porosity, when increasing either Al/P or the water content. On a structural point of view, a combined study by XRD and FTIR showed that:

(i) For Al/P = 1 with different water contents, the network is mainly based on Al-O-P bonds with an hydrated silica network across the different compositions. The contribution

of each network can be continuously modified by the addition of water, thus giving a good control over the properties of the resulting geopolymer.

(ii) For variable Al/P, the same networks as in (i) are identified. However, the presence of unreacted metakaolin modifies the control over their distribution, making it more challenging. Moreover, the molecular interactions will favor the formation of Si-O-P and Si-O-Al bonds.

In all the cases, this study showed that both the water amount and the Al/P compositions are parameters that can be used to decrease the viscosity of the initial reactive mixture. However, their noticeable influence on the structure and properties of the resulting geopolymers is to be carefully monitored.

Table 1: viscosity and setting time observed for the different samples.

Samples		**[P] (M)**	**H_2O (mol%)**	**Viscosity (Pa.s)**	**Setting time (min)**
Al/P = 1	**R**	6.49	0.45	30.0	46
	R-1.1	5.97	0.50	14.5	46
	R-1.2	5.57	0.55	4.0	48
	R-1.3	5.14	0.60	1.7	63
	R-1.4	4.85	0.63	1.4	56
	R-1.5	4.51	0.68	0.6	69
Variable Al/P	**0.9**	7.23	0.39	38.6	68
	1.1	5.82	0.49	19.1	32
	1.2	5.28	0.52	17.2	35
	1.5	4.23	0.58	5.6	17
	1.8	3.50	0.62	2.2	9

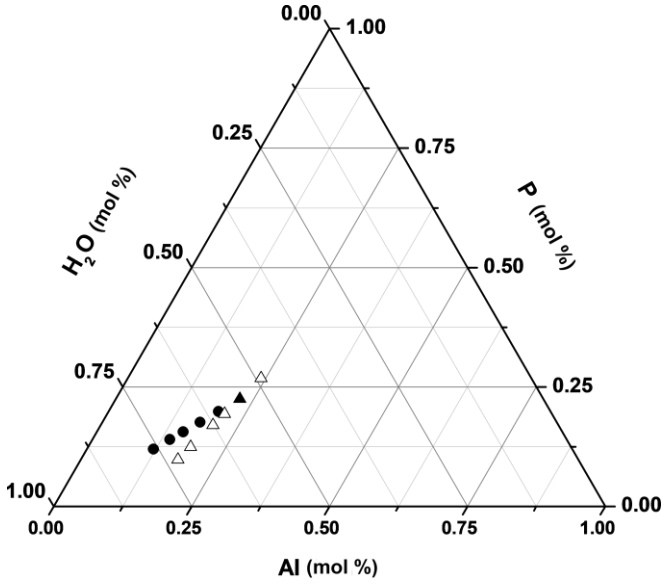

Figure 1: composition of the reactive mixture for samples with (●) Al/P=1 and a variable water content, (△) a variable Al/P ratio and (▲) the reference sample.

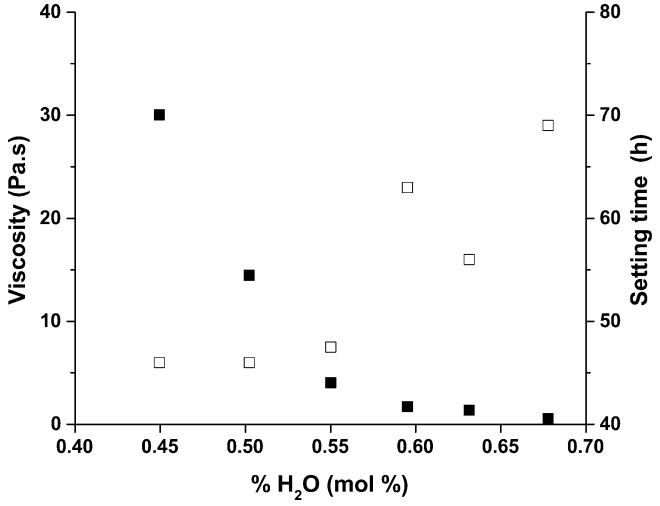

Figure 2:(□) viscosity (±1%) and (■) setting time (±1h) as a function of the percentage of water for the different formulations.

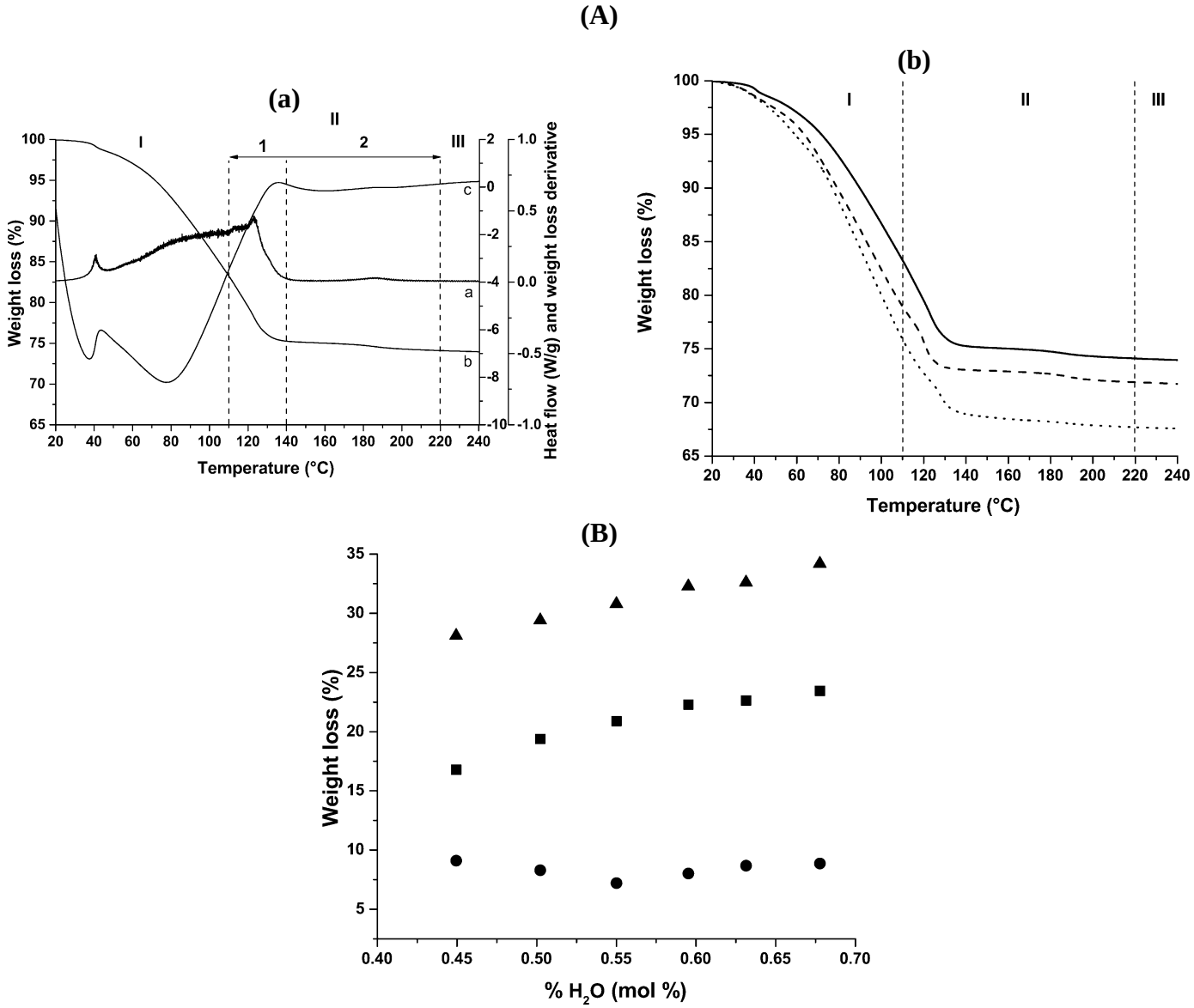

Figure 3: (A) (a) thermal analysis (weight loss (b), derivative (a) and heat flow (c)) of the R-1.2 sample and (b) thermograms of (—) R, (– –) R-1.2 and (…) R-1.5 samples. (B) weight loss measured during steps I (RT to 100°C) (■), II (110 to 220°C) (●), and total weight loss (RT to 1000°C) (▲) as functions of the water content introduced.

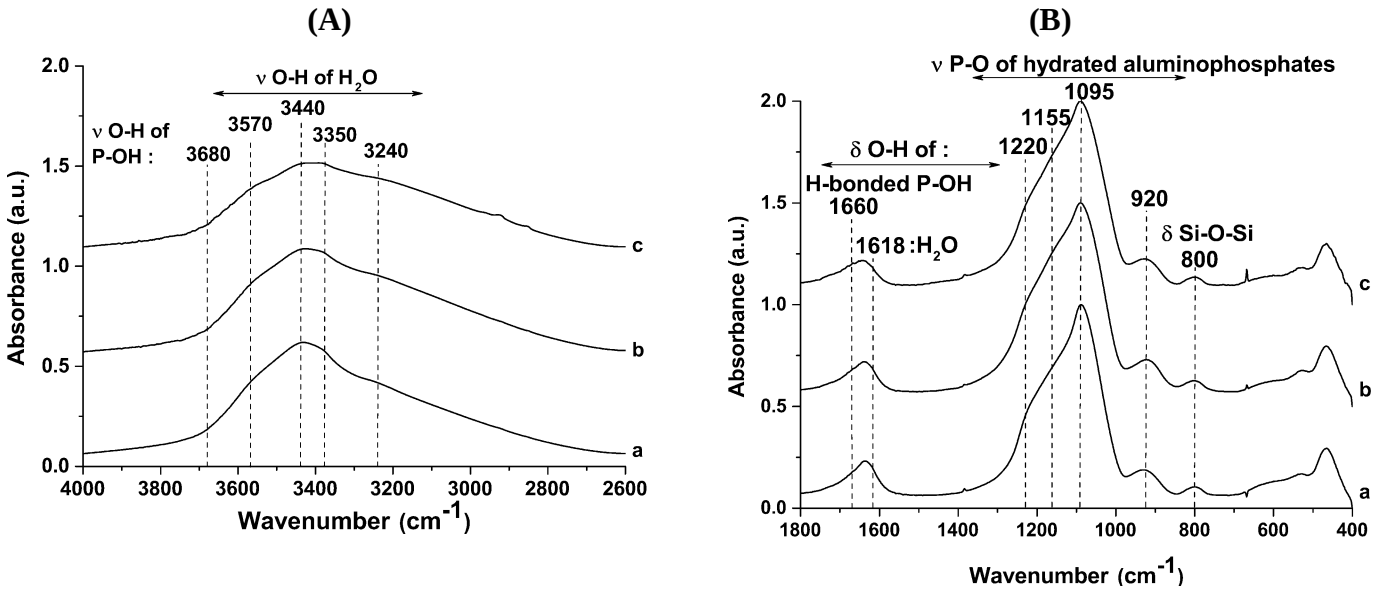

Figure 4 : (A) FTIR spectra between (a) 4000 and 2600 cm^{-1} and (B) 1800 and 400 cm^{-1} for (a) R, (b) R-1.2 and (c) R-1.5 samples.

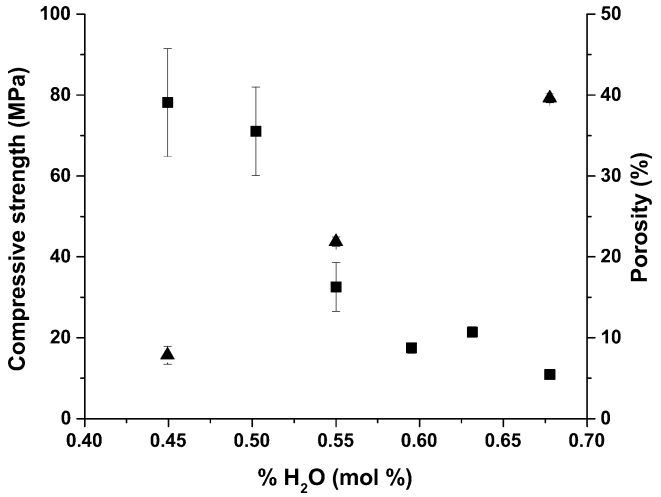

Figure 5: compressive strength (■) and porosity (▲) as functions of the water content.

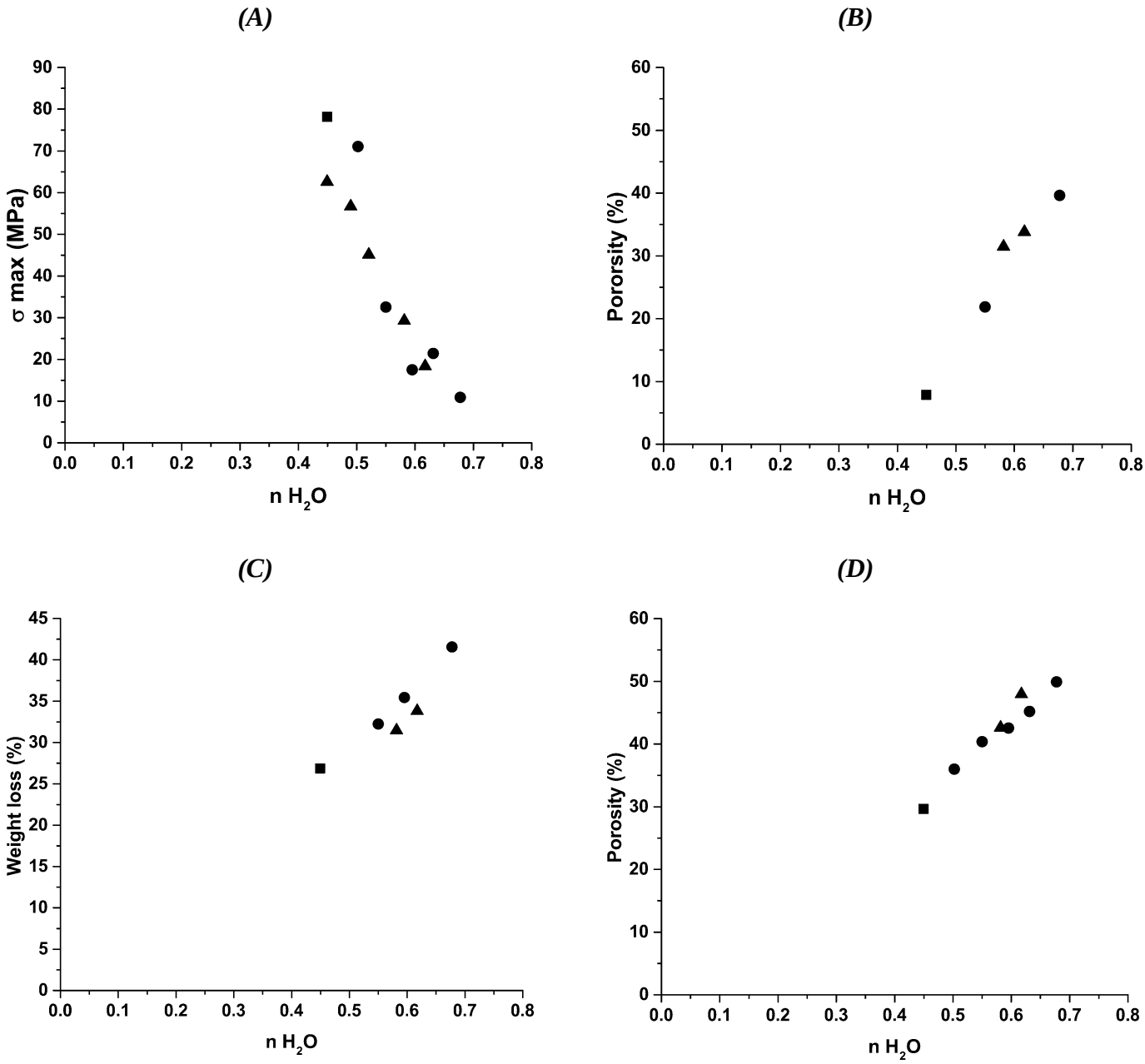

Figure 6: (A) compressive strength, (B) porosity, (C) water loss after thermal treatment at 250°C, and (D) porosity after thermal treatment at 250°C, for the samples (■) R, (●) Al/P = 1 and variable water and (◢) variable Al/P.

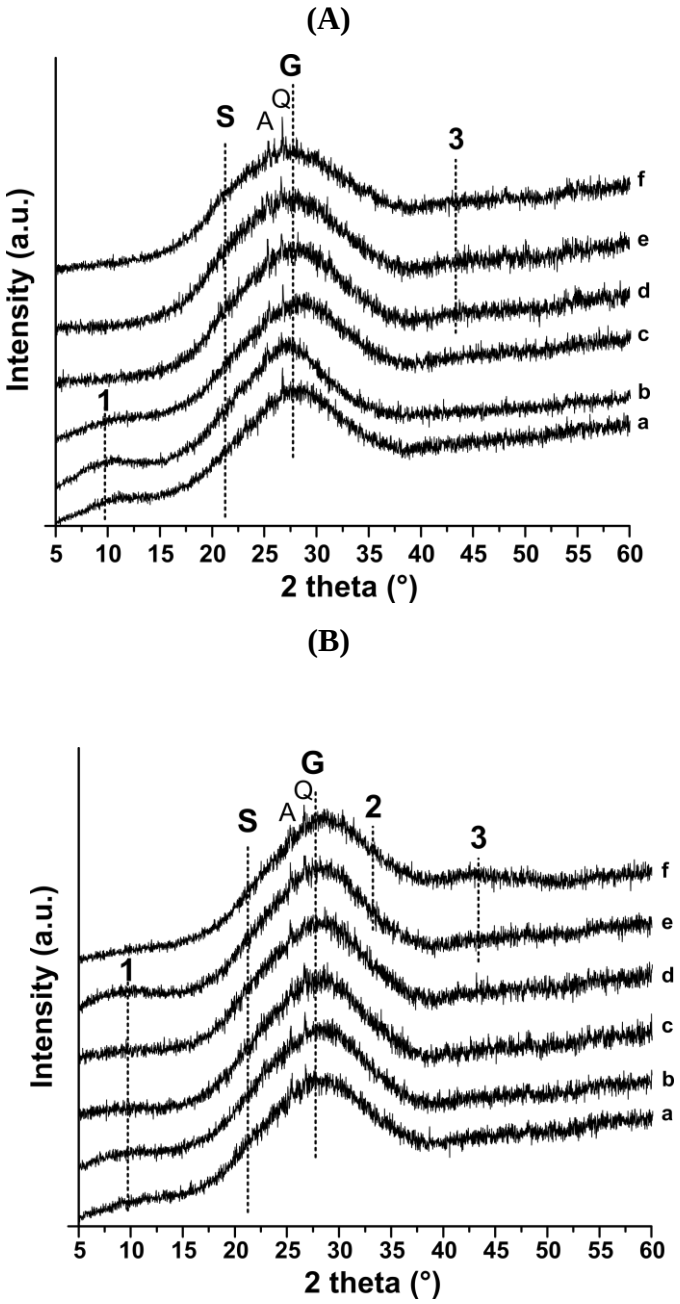

Figure 7:(A) diffraction diagrams of samples with various Al/P (a) 0.9, (b) 1, (c) 1.1, (d) 1.2, (e) 1.5, (f) 1.8 and (B) diffraction diagrams of samples with Al/P = 1 and a variable amount of water (a) R, (b) R-1.1, (c) R-1.2, (d) R-1.3, (e) R-1.4, (f) R-1.5. The positions of crystalline anatase (A: 01-071-1166) and quartz (Q: 00-046-1045) are shown, as well as the positions of the different amorphous contributions identified (S, G and peaks 1, 2 and 3).

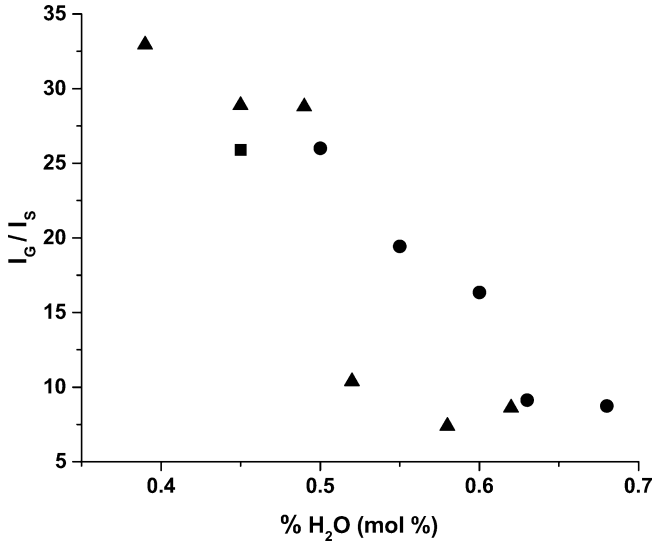

Figure 8: I_G/I_S of (■) R, (●) Al/P = 1 and variable water, and (▲) Al/P variable plotted as functions of the water content.

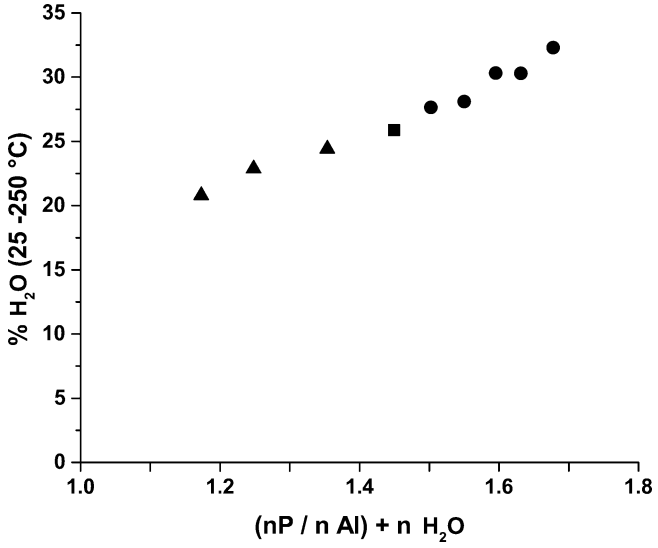

Figure9: water content determined by thermal analysis as a function of $\frac{nP}{nAl} + n_{H2O}$ with (■) R, (●) Al/P = 1 and variable water addition, and (▲) Al/P variable.

(A)

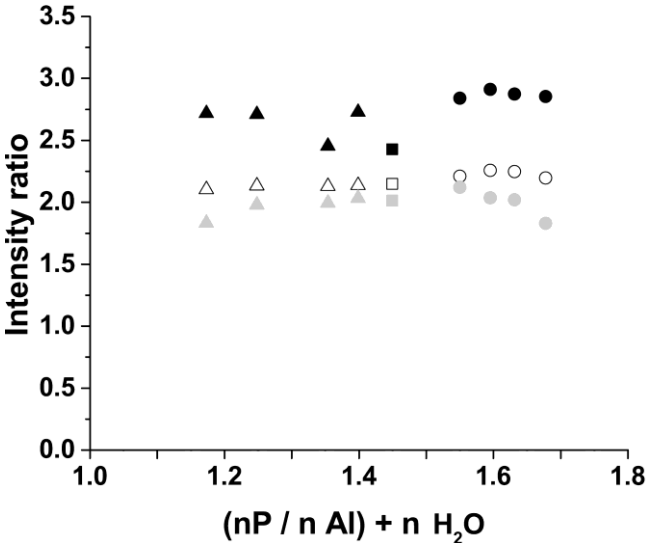
Intensity ratio
3.5
3.0
2.5
2.0
1.5
1.0
0.5
0.0
1.0
1.2
1.4
1.6
1.8
(nP / n Al) + n H2O

(B)

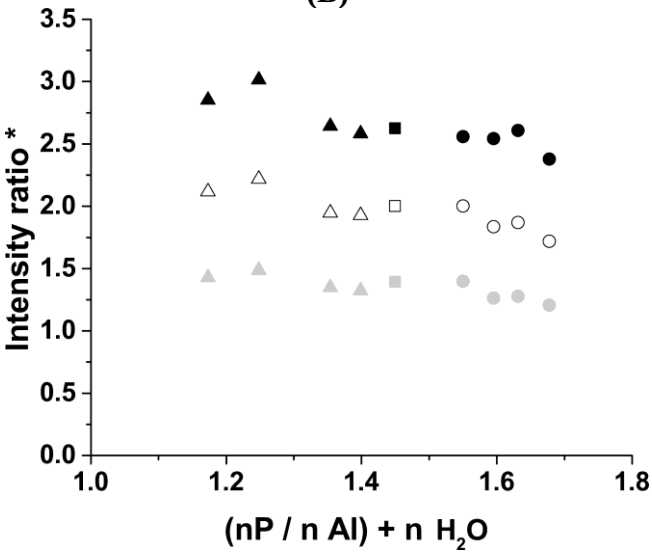
Intensity ratio *
3.5
3.0
2.5
2.0
1.5
1.0
0.5
0.0
1.0
1.2
1.4
1.6
1.8
(nP / n Al) + n H2O

(C)

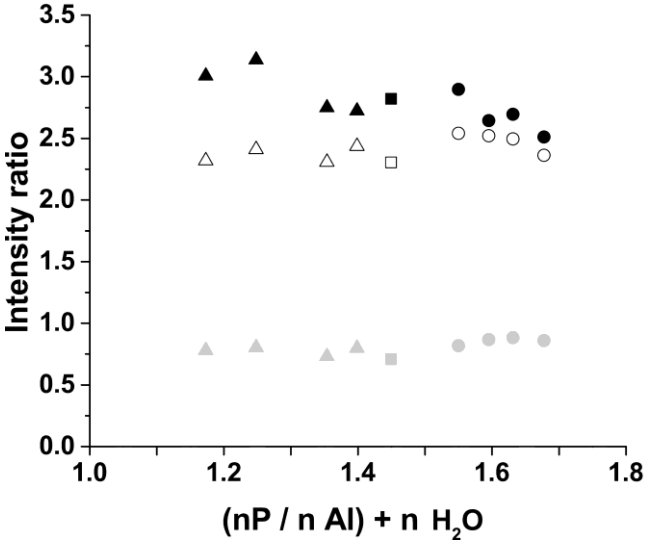
Intensity ratio
3.5
3.0
2.5
2.0
1.5
1.0
0.5
0.0
1.0
1.2
1.4
1.6
1.8
(nP / n Al) + n H2O

Figure 10: evolution of the intensity of characteristic FTIR contributions (identified by their positions in cm^{-1}) of (A) silicate hydrated networks (□■) SiO-H (asym 3530 - sym 3440) and (■)H_2O 3240 cm^{-1}, (B) phosphate networks (■) v Al-O-P 1220, (■, □) v P-O asym 1095 -sym 1155 cm^{-1}, and (C) summary (□) hydrated Al-O-P at 3350, (■) PO-H at 1640 and (■) Si-O-P at 1206 cm^{-1}. These evolutions are displayed for (■) R, (●) Al/P = 1 and variable water addition, and (▲) Al/P variable samples as functions of the parameter $\frac{nP}{nAl} + n_{H20}$. In (B), (*) intensity divided by 2.

References

[1] J. Davidovits, Geopolymers, J. Therm. Anal. 37 (8) (1991) 1633–1656.
[2] M. Irfan Khan, K. Azizli, S. Sufian, A. Sada Khan, H. Ullah, Z. Man, World Sustainability Forum, Conference Proceedings Paper (2014).
[3] A. Gharzouni, E. Joussein, B. Samet, S. Baklouti, S. Rossignol, Effect of the reactivity of alkaline solution and metakaolin on geopolymer formation , J. Non-Cryst. Solids 410 (2015) 127-134.
[4] D. S. Perera, Relative strengths oh phosphoric acid-reacted and alkali-reacted metakaolin materials, J Mater Sci 43 (2008) 6562–6566.
[5] H. K. Tchakouté et C. H. Rüscher, Mechanical and microstructural properties of metkaolin-based geopolymer cements from sodium waterglass and phosphoric acid solution as hardeners: a comparative study, Applied Clay Science 140 (2017) 81-87.
[6] V. Mathivet, J. Jouin, A. Gharzouni, I. Sobrados, H. Celerier, S. Rossignol, M. Parlier, Acid-based geoolymers: understanding of the structural evolutions during consolidation and after thermal treatments, Journal of Non-Crystalline Solids 512 (2019) 90–97.
[7] H. Celerier, J. Jouin, A. Gharzouni, V. Mathivet, I. Sobrados, N. Tessier-Doyen, S. Rossignol, Relation between working properties and structural properties from ^{27}Al, ^{29}Si and ^{31}P NMR and XRD of acid-based geopolymers from 25 to 1000°C, Materials Chemistry and Physics 228 (2019) 293-302.
[8] S. Louati, S. Baklouti, B. Samet, Acid based geopolymerization kinetics: effect of clay particle size, Appl. Clay Sci. 132–133 (2016) 571–578.
[9] H. Celerier, J. Jouin, V. Mathivet, N. Tessier-Doyen, S. Rossignol, Composition and properties of phosphoric acid-based geopolymers, J. Non-Cryst. Solids 493 (2018) 94–98.
[10] K.K. Tchakouté, C Rusher, E. Kamseu, J Djobo and C. Leonelli, The influence of gibbsite in kaolin and the formation of berlinite on the properties of metakaolin-phosphate –based geopolymer cements, Mat Chem Phys. 197 (2017) 280-288.
[11] H.K. Tchakouté, C H. Ruscher, E. Kamseu, F. Andreola and C Leonetti, Influence of the molar concentration of phosphoric acid solution on the properties of metakaolin phosphate based geopolymer cements. Applied Clay Science 147 (2017) 184-194.
[12] T Dong, Y Zhang, Y Jiang, G. Zhao, X Yu, Workability and mechanical property of metakaolin phosphate aced bases geopolymer, IOP conf Earth and environnemental Science 267 (2019) 022002.

[13] M. Zibri, B. Samet, S. Baklouti, Mechanical, microstructural and structural investigation of phosphate based geopolymers with respect to P/Al molar ratio, Journal of Solid State Chemistry 281 (2020) 12105.
[14] D. Karbalaei Saleh, H. Abdollahi, M. Noaparast and A. Fallah Nosratabad, Dissolution of aluminium from metakaolin with oxalic, citric and lactic acids, Clays mineral 54 (2019) 209-217.
[15] C. Belver and MA Vicente, Porous silica by acid leaching of metakaolin, Materials syntheses: a practical guide (2008) 47-51.
[16] J. Davidovits, Geopolymer chemistry and applications, Third ed., Institute Geopolymer, Saint-Quentin, France, 2011 (612 p).
[17] A Karsiki, Aluminosilicate phosphate cements a critical review, Advances in applied ceramics, Advances in Applied Ceramics, 118(5) (2019) 274-286.
[18] A. Gharzouni, I. Sobrados, E. Joussein, S. Baklouti, S. Rossignol, Control of polycondensation reaction generated from different metakaolins and alkaline solutions, J. Ceram. Sci. Technol 8 (2017) 365-376.
[19] O. Masson, PEAKOC profile fitting software v1.0, 2006, access at http://www.esrf.eu/Instrumentation/software/data-analysis/OurSoftware/PEAKOC.
[20] J Januari, H. Fansuri and MA. Bakri, The relationship between Vickers microhardness and compressive strength of functional surface geopolymers, AIP Conference Proceedings, 020170 (2017) 1885.
[21] C N Bwa, HK Tchakouté, D. Fotio, CH Rusher, E Kamseu, C Leonelli, Water resistance and thermal behavior of metakaolin based geopolymer cements, 6 (3) (2018) 271-283.
[22] D Spspielbauer, G. A. H. Mekhemer, T. Riemer, M. I. Zaki, and H. Knözinger, J. Phys. Chem. B, 101(1997) 4681-4688.
[23] K. Hadjiivanov, Chapter Two: Identification and characterization of surface hydroxyl groups by infrared spectroscopy, Advances in Catalysis 57 (2017) 99-318. editor John Cross.
[24] R. Frost, R. Scholz, F. Belotti, A. López, F. Theiss, A vibrational spectroscopic study of the phosphate mineral vantasselite $Al_4(PO_4)_3(OH)_3$; 9 H_2O, Spectrochimi. Acta, Part A 147 (2015) 185.
[25] B. Boonchom, S. Kongtaweelert, Study of kinetics and thermodynamics of the dehydration reaction of $AlPO_4$, H_2O, J. Therm. Anal. Calorim. 99 (2010) 531-538.
[26] J.F. Agassant, P. Avenas, J.P. Sergent, B. Vergnes, M. Vincent, Mise en forme des polymères : approche thermomécanique de la plasturgie, Lavoisier (2014).
[27] A.Wurger, Thermal non-equilibrium transport in colloids, Reports on Progress in Physics 73 (12) (2010), 126601 (35p).
[28] L. Weng and K. SagoeKrensil, Dissolution processes, hydrolysis and condensation reactions during geopolymer synthesis: Part I-Low Si/Al ratio systems, J Mater Sci 42 (2007) 2997–3006.
[29] P Steins, Influence des paramètres de formulation sur la texturation et la structuration des géopolymères, Thesis of University of Limoges (2014).
[30] A. Favier, Mécanisme de prise et rhéologie de liants géopolymères modèles, Thesis of University Paris Est (2013).
[31] V. Benavent, P. Steins, I. Sobrados, J. Sanz, D. Lambertin, F. Frizon, S. Rossignol, Impact of aluminum on the structure of geopolymers from the early stages to consolidated material, Cement and Concrete Research 90 (2016) 27-35.
[32] H. Rohee, J. Jouin, V. Mathivet, N. Tessier Doyen, S. Rossignol, Composition and properties of phosphoric acid-based geopolymers, J. Non Cryst. Solids, 493 (2018) 94-98.
[33] A. Gharzouni, L. Vidal, N. Essaidi, E. Joussein, S. Rossignol, Recycling of geopolymer waste: influence on geopolymer formation and mechanical properties, Mater. Des. 94 (2016) 221–229.

[34] P. Deshmuk, J. Bhatt, D. Peshwe, S. Pathak, Determination of silica activity index and XRD, SEM and EDS studies of amorphous SiO_2 extracted from rice husk ash, Trans. Indian Inst. Metals 65 (2012) 63–70.
[35] M.D. Shannon, J.L. Casci, P.A. Cox, S.J. Andrews, Structure of the two-dimensional medium-pore high-silica zeolite NU-87, Nature 353 (1991) 417–420.
[36] L. Guth, D. Jordan, A. Kalt, B. Perati, R. Wey, Un nouveau type de silice hydratée crystallisée, de formule $H_2Si_3O_7$ C.R. Acad. Sci. Paris 285 (1977) 1367–1370.
[37] J.P. Gevaudan, J.D. Wallat, B. Lama, W.V. Srubar, PVA an PEG assisted sol-gel synthesis of aluminosilicate precursors for N-A-S-H geopolymer cements, Journal of the American Ceramic Society 103 (2) (2020) 859-877.
[38] E.G. Derouane, J.G. Fripiat, R. Von Ballmoos, Quantum mechanical calculations on molecular sieves. 2. Model cluster investigation of silicoaluminophosphate, J.Phys. Chem. 94 (1990) 1687-1692.
[39] T. Hanada, A. Ando, S. Tanabe, N. Soga, Properties and network constitution of rf-sputtered amorphous films in the system silicon dioxide-aluminum orthophosphate, J. Am. Ceram. Sci. 75 (12) (1992) 3417-3416.